Thermal expansion and magnetostriction of $CeAl_2$

Eric Fawcett
Physics Department and Scarborough College, University of Toronto, Toronto, Canada M5S 1A7

V. Pluzhnikov
Institute of Low Temperature Physics and Engineering, Academy of Sciences of the Ukrainian Soviet Socialist Republic, Lenin Prospect 47, Kharkov 310164, U.S.S.R.

H. Klimker
Nuclear Research Centre-Negev, P.O.B. 9001, Beer Sheva, Israel
(Received 19 March 1990)

The thermal expansion and magnetostriction for various configurations of strain and field direction in single crystals of $CeAl_2$ are measured in the temperature range 1.2 to 4.2 K in magnetic fields up to 10 T. A phase diagram is constructed, comprising the antiferromagnetic and high-field phases. The temperature dependence of the magnetostriction constants is determined for the high-field phase in a field of 10 T relative to the zero-field antiferromagnetic state. The paramagnetostriction coefficients are measured at a temperature of 4.2 K in fields up to 5 T.

INTRODUCTION

The cubic Laves-phase compound $CeAl_2$ is a periodic Kondo system,[1] or Kondo lattice, having thermal[2] and magnetic[3] properties of special interest. The Kondo interaction of a single Ce site is dominated by the Ruderman-Kittel-Kasuya-Yosida interaction between the sites, resulting in low-temperature magnetic ordering, with a single-ion Kondo temperature,[4] $T_N = 5 \pm 2$ K. Below the Néel temperature, $T_N = 3.9$ K, a sinusoidal incommensurate spin-density wave was observed by neutron diffraction.[5] The magnetic structure is complex, with a single crystal comprising 24 single-wave-vector domains.[6]

The magnetoelastic coupling is strong in $CeAl_2$, especially for shear strain.[7] Studies of the direct pressure dependence of the Néel temperature T_N have yielded conflicting results, even as to the sign of the effect.[8,9] Schefzyk *et al.*[10] measured the thermal expansion and specific heat at zero pressure of single crystal and polycrystalline $CeAl_2$, and found clear evidence for two transitions between temperatures 3.7 and 3.9 K. The jump in the thermal expansivity, and therefore the pressure dependence, was opposite in sign at these two transitions, while the absolute magnitude deduced by means of the Ehrenfest relation was in rough agreement with the direct pressure results.

There is a discrepancy between the positive sign of the thermal expansivity α in the antiferromagnetic phase observed by Schefzyk *et al.*[10] and the negative α reported by previous workers.[11–13] As reported previously by one of the authors,[14] the present results confirm the earlier work, and thus indicate an error by Schefzyk *et al.*[10] in determining the sign of α.

The thermal expansion[11] and magnetostriction[12] of polycrystalline $CeAl_2$ below the Néel temperature provide evidence for a field-induced metamagnetic phase transition, which was observed first in the high-field magnetization.[3] The strain is an approximately quadratic function of field at low fields, while it begins to approach saturation at high fields, and the point of inflection of the curve of strain versus field is taken to mark the phase transition.[11] The nature of the anisotropy of the magnetostriction[12] shows that the distortive strain is much larger than the volume strain, as expected from the strong field dependence of the shear elastic constant.[7]

The high-field phase has unknown magnetic structure. The phase transition from the antiferromagnetic to the high-field phase is marked also by a sharp drop in the resistivity[15,16] with increasing field. A similar effect[17] occurs in the Kondo lattice $CePb_3$.

Steglich *et al.*[4] have reviewed the experimental situation of this unusual compound, which is the first metal to be found in which the Kondo effect and long-range magnetic order coexist. It has been suggested[15] that the metamagnetic phase corresponds to the freezing out of spin degrees of freedom by a high magnetic field, which reduces the resistivity by removing the scattering of electrons by spin-flop or by spin-density-wave excitations.[18]

We have measured the thermal expansion and magnetostriction of single crystals of $CeAl_2$ in magnetic fields up to 10 T, for various configurations of strain and field throughout the antiferromagnetic range of temperatures, and also in the paramagnetic phase at temperature 4.2 K, just above the Néel temperature. For some configurations the field-induced phase transition is marked by sharp peaks in the thermal expansivity or magnetostriction, and accordingly we have been able to map the phase diagram quite accurately. The high-field magnetostriction constants for a field of 10 T are determined as a function of temperature from 1.2 to 4.2 K. The paramagnetostriction coefficients for fields up to about 5 T at temperature 4.2 K are also measured.

EXPERIMENT

Two single-crystal samples of $CeAl_2$ were spark cut from a boule[19] comprising several crystallites of different orientation. The samples were of dimensions 3 to 4 mm and had plane-parallel faces perpendicular to the [100] and [110] axes, to an accuracy of about 3°.

The thermal expansion and magnetostriction were measured by a capacitance method.[20] Each sample was glued with epoxy to the base of a beryllium-copper capacitance dilatometer cell. The capacitance of the cell was measured with a General Radio 1616 three-terminal capacitance bridge, as field was varied by a 10-T General Electric superconducting solenoid, and temperature was varied in the range 1.2 to 4.2 K by pumping liquid helium.

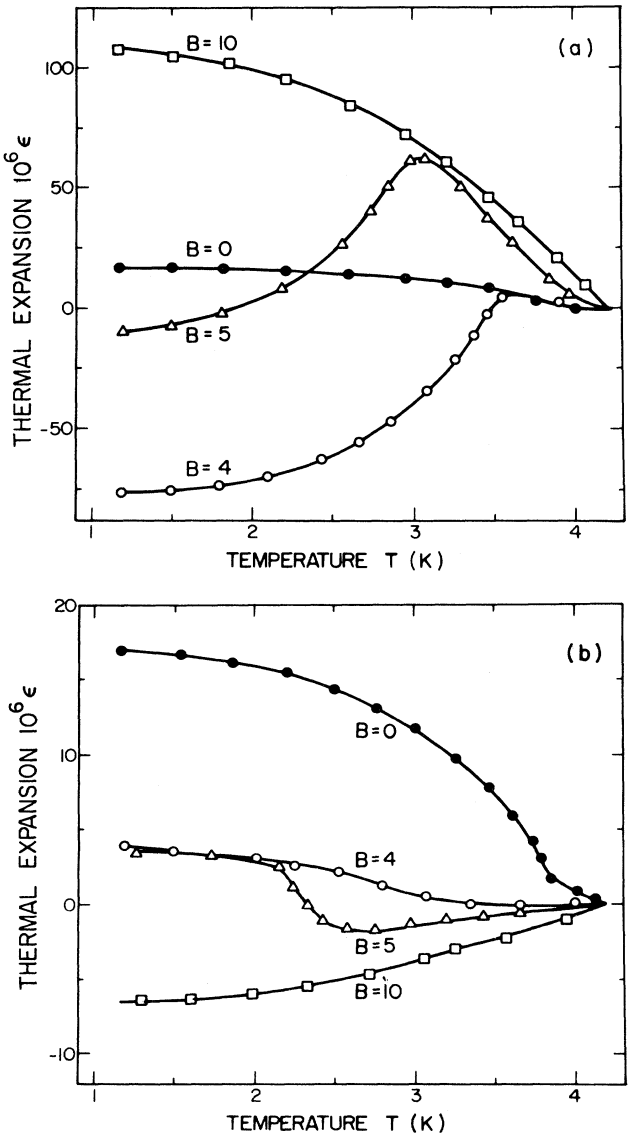

FIG. 1. Thermal expansion of $CeAl_2$ measured along a cube axis in magnetic fields B in units of T: (a) longitudinal with field parallel to strain (line 1 of Table I); (b) transverse with field along a cube axis perpendicular to strain (line 2 of Table I).

RESULTS

The thermal expansion and magnetostriction for various configurations of the strain direction ϵ and the magnetic field direction **B** are shown in Figs. 1–7. The configurations of ϵ and **B** relative to the crystal axes are given in Table I. For each configuration the thermal expansion was measured for several values of the magnetic field from zero to $B=10$ T, but only the data and curves for $B=0$, 4, 5, and 10 T are shown in the figures. The magnetostriction was measured at several temperatures in the range $T=1.2$ to 4.2 K, but only the data and curves for $T=1.5$, 3.0, and 4.2 K are shown.

The thermal expansivity in zero field is negative, as is shown in Figs. 1(a), 1(b), 4(a), 5(a), 6(a), and 7(a). It appears, as seen most clearly in Fig. 1(b), that the strain, $\epsilon=\Delta l/l$, shows no discontinuity at the Néel temperature, $T_N=3.85\pm0.1$ K, but the thermal expansivity, $\alpha=d\epsilon(T)/dT$, is discontinuous, with

$$\Delta\alpha=\lim_{T\to T_N}[\alpha_- - \alpha_+] =(-15\pm3)\times10^{-6}\ \mathrm{K}^{-1}\ . \quad (1)$$

In Eq. (1) we follow the unusual convention that the subscript $+(-)$ for α refers to temperatures above (below) the Néel temperature, and that the sign of the discontinuity $\Delta\alpha$ is that of the low-temperature ordered phase relative to the high-temperature disordered phase.

The longitudinal magnetostriction is large and positive

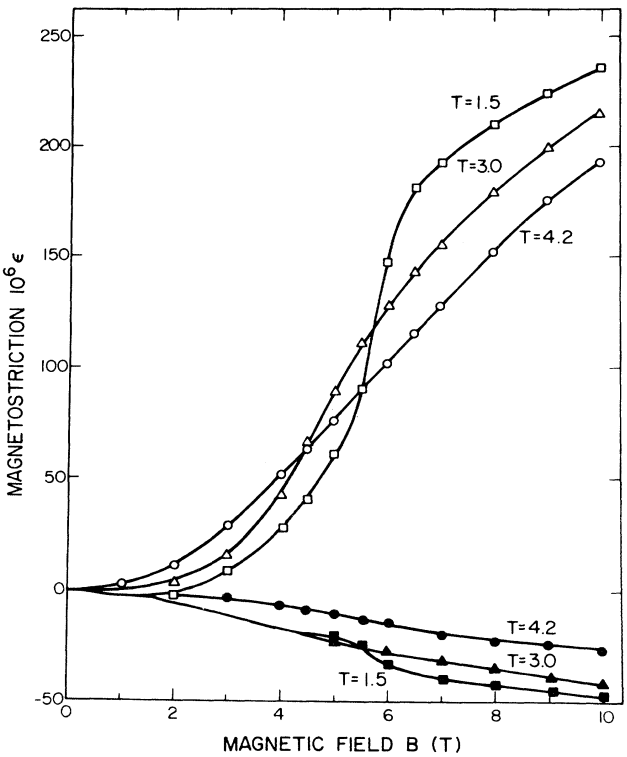

FIG. 2. Longitudinal (upper curves and line 1 of Table I) and transverse (lower curves and line 2 of Table I) magnetostriction of $CeAl_2$ at temperature T in units of K for field and strain along cube axes.

[Figs. 2 (upper curves) and 4(b)]. The transverse magnetostriction is relatively small and negative for field **B** along a cube axis [Figs. 2 (lower curves) and 7(b)]. The resultant volume magnetostriction is large and positive at all temperatures for fields greater than about 5 T (Fig. 3). Below the Néel temperature the volume magnetostriction is small and negative at low fields and changes sign with increasing field.

In high magnetic fields the longitudinal thermal expansivity is negative [Figs. 1(a) and 4(a)], while the transverse thermal expansivity is positive [Figs. 1(b), 5(a), and 6(a)]. At some intermediate fields, the thermal expansivity changes sign with increasing temperature [Figs. 1(a), 1(b), 4(a), 5(a), and 6(a)].

We define the transition with increasing field from the antiferromagnetic phase to the high-field metamagnetic phase, following Croft *et al.*[11], by the inflection point in the thermal expansion curve [Figs. 1(a) and 4(a)], i.e., the temperature at which the thermal expansivity is a maximum. The magnetostriction curves provide in most cases however a clearer demarcation of the phase boundary, either through an inflection where the differential magnetostriction is a maximum [Figs. 2, 4(b), 5(b), and 6(b)], or a peak in the magnetostriction [Fig. 7(b)].

The resultant phase diagram shown in Fig. 8 is in reasonably good agreement with those given by Croft *et al.*[11] and Lapierre *et al.*[16] For field **B** along the cubic and twofold symmetry axes, the phase boundary coincides with that found by these authors for a polycrystalline sample. For **B** along a threefold symmetry axis the phase boundary diverges below about temperature, $T=3$ K, and at the lowest temperature, $T \lesssim 1.5$ K, the sample enters the high-field phase at a field about 1 T lower than

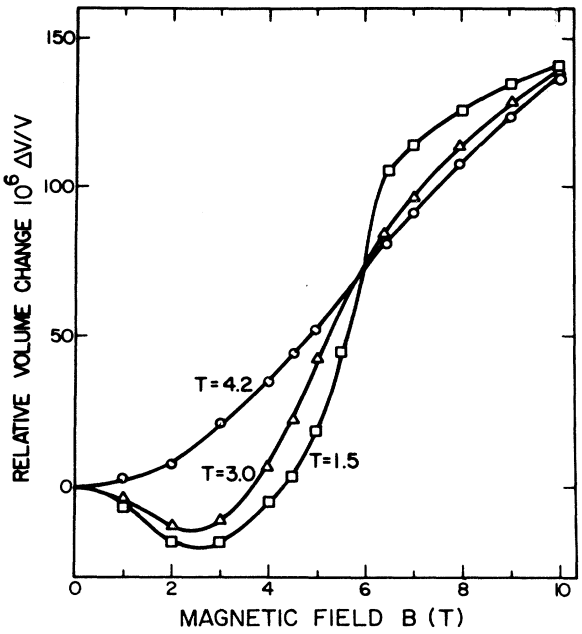

FIG. 3. Volume magnetostriction of $CeAl_2$ for field along a cube axis.

for the other field directions. This behavior is consistent with the observed anisotropy of the magnetization curves.[3]

The extrema in the magnetostriction seen in the antiferromagnetic phase at temperatures 1.5 K and 3.0 K for relatively low fields, $B \simeq 10$ T to 15 T, directed along lower symmetry axes [Figs. 4(b), 5(b), and 6(b)] provide further evidence for a domain-reorientation line on the

TABLE I. Paramagnetostriction of $CeAl_2$ at temperature 4.2 K in magnetic fields up to $B \sim 5$ T. The configurations of the strain direction ϵ and field direction **B** refer to either or both the magnetostriction and thermal expansion figures.

Line	Configuration (direction cosines) ϵ	**B**	$\frac{\epsilon(B)}{B^2}$ [Eq. (3)]	Fig.	$\frac{\epsilon}{B^2}(10^{-8}T^{-2})$
1	(0,0,1)	(0,0,1)	$\frac{1}{3}L_V+\frac{2}{3}L_{100}$	1(a) and 2 (upper curves)	300
2	(1,0,0)	(0,0,1)	$\frac{1}{3}L_V$	1(b) and 2 (lower curves)	−50
3	$\left[\frac{1}{\sqrt{2}},\frac{1}{\sqrt{2}},0\right]$	$\left[\frac{1}{\sqrt{2}},\frac{1}{\sqrt{2}},0\right]$	$\frac{1}{3}L_V+\frac{3}{4}L_{100}+\frac{3}{4}L_{111}$	4(a) and 4(b)	1200
4	$\left[\frac{1}{\sqrt{2}},\frac{-1}{\sqrt{2}},0\right]$	$\left[\frac{1}{\sqrt{2}},\frac{1}{\sqrt{2}},0\right]$	$\frac{1}{3}L_V+\frac{3}{4}L_{100}-\frac{3}{4}L_{111}$	5(a) and 5(b)	−920
5	$\left[\frac{1}{\sqrt{2}},\frac{-1}{\sqrt{2}},0\right]$	$\left[\frac{1}{\sqrt{3}},\frac{1}{\sqrt{3}},\frac{1}{\sqrt{3}}\right]$	$\frac{1}{3}L_V+\frac{1}{2}L_{100}-\frac{1}{2}L_{111}$	6(a) and 6(b)	−850
6	$\left[\frac{1}{\sqrt{2}},0,\frac{1}{\sqrt{2}}\right]$	(0,0,1)	$\frac{1}{3}L_V+\frac{2}{3}L_{100}$	7(a), $\epsilon(B)$ not measured	
7	$\left[\frac{1}{\sqrt{2}},\frac{1}{\sqrt{2}},0\right]$	(0,0,1)	$\frac{1}{3}L_V$	7(b)	−30
8	(0,0,1)	$\left[\frac{1}{\sqrt{2}},\frac{1}{\sqrt{2}},0\right]$	$\frac{1}{3}L_V$	10, hysteresis	

phase diagram, as suggested by the behavior of the magnetoresistance in polycrystalline samples.[17]

The magnetostriction in the highest field, $B=10$ T, that we used to produce the metamagnetic phase, may be described approximately by the standard expression[21] employing three temperature-dependent magnetostriction constants λ_i

$$\epsilon(T)=\frac{\Delta l(T)}{l}=\tfrac{1}{3}\lambda_v+\tfrac{3}{2}\lambda_{100}\sum_i \alpha_i^2\beta_i^2+3\lambda_{111}\sum_{i\neq j}\alpha_i,\alpha_j\beta_i\beta_j\ , \quad (2)$$

where α_i and $\beta_i (i=1,2,3)$ are the direction cosines of the strain direction ϵ and the magnetic-field direction **B**, respectively.

The volume magnetostriction constant λ_V may be determined from the values of ϵ for $B=10$ T in Fig. 2 (lower curves) and Fig. 7(b), which agree within about $\pm 10\%$. The tetragonal shear constant λ_{100} may then be determined from Fig. 2 (upper curves), and the trigonal shear constant λ_{111} by substituting the values of ϵ for $B=10$ T in Figs. 4(b) and 5(b).

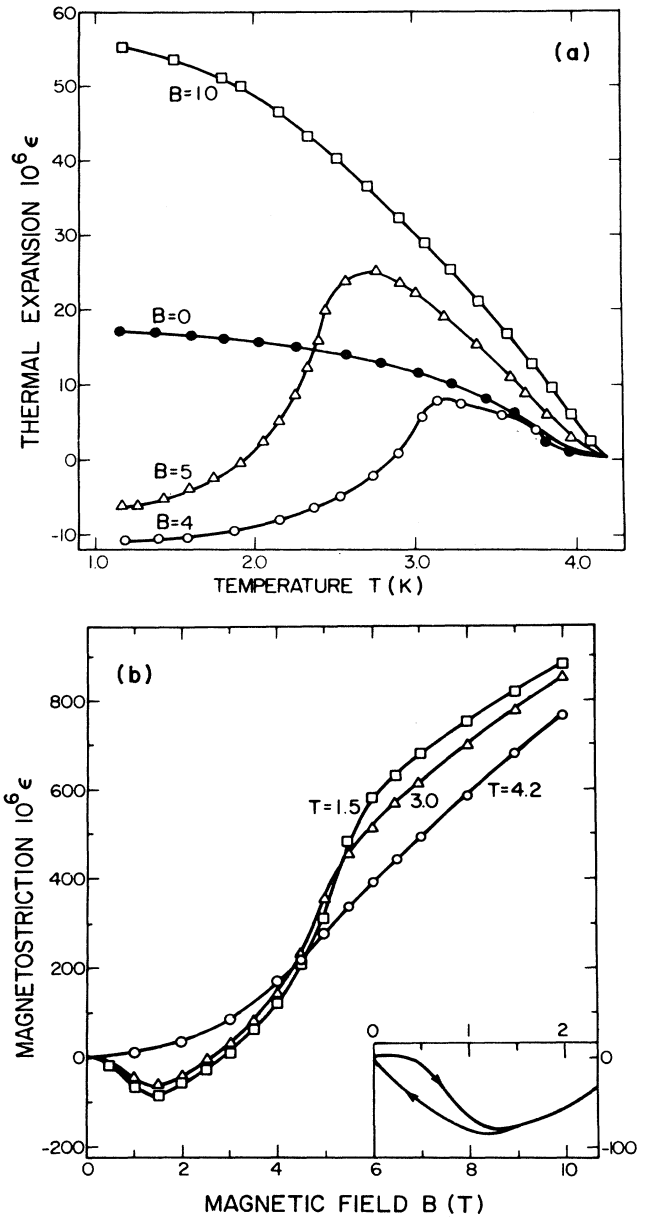

FIG. 4. (a) Thermal expansion of $CeAl_2$ with both magnetic field B in units of T and strain along the same twofold symmetry axis; (b) magnetostriction of $CeAl_2$ at temperature T in units of K for the same configuration (line 3 of Table I), with hysteretic behavior at $T=1.5$ K shown in the insert.

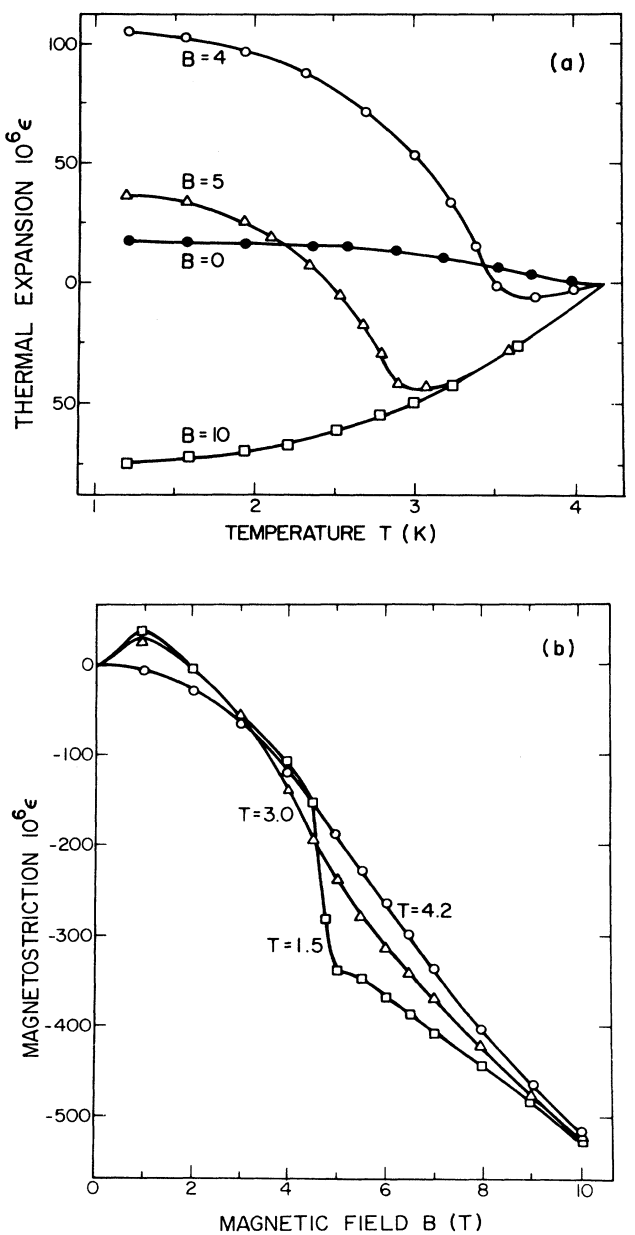

FIG. 5. (a) Thermal expansion of $CeAl_2$ with magnetic field B in units of T and strain along different twofold symmetry axes; (b) magnetostriction of $CeAl_2$ at temperature T in units of K for the same configuration (line 4 of Table I).

The resultant values of λ_V, λ_{100} and λ_{111} are plotted as functions of temperature in Fig. 9. They may be checked by calculating the values of ϵ for $B=10$ T, corresponding to the configuration of Fig. 6(b). The calculated values of ϵ -515×10^{-6}, -490×10^{-6}, and 410×10^{-6} at temperatures 1.5, 3.0, and 4.2 K, respectively, are to be compared with the measured values -535×10^{-6}, -528×10^{-6}, and 520×10^{-6}. The fit is not good, but one should note that Eq. (2) is intended to fit the anisotropy of the saturation magnetostriction of a ferromagnet, whereas in a field of only $B=10$ T the magnetostriction of the metamagnetic phase of $CeAl_2$ is by no means saturated. Thus, the upper curves in Fig. 2, where the magnetostriction is essentially equal to $(3/2)\lambda_{111}$, show that both magnetostriction constants are still increasing quite rapidly with field. It was considered inappropriate accordingly to use an elaborate fitting procedure to determine the optimum values of the magnetostriction constants, and the values plotted in Fig. 9 were determined by the procedure described above.

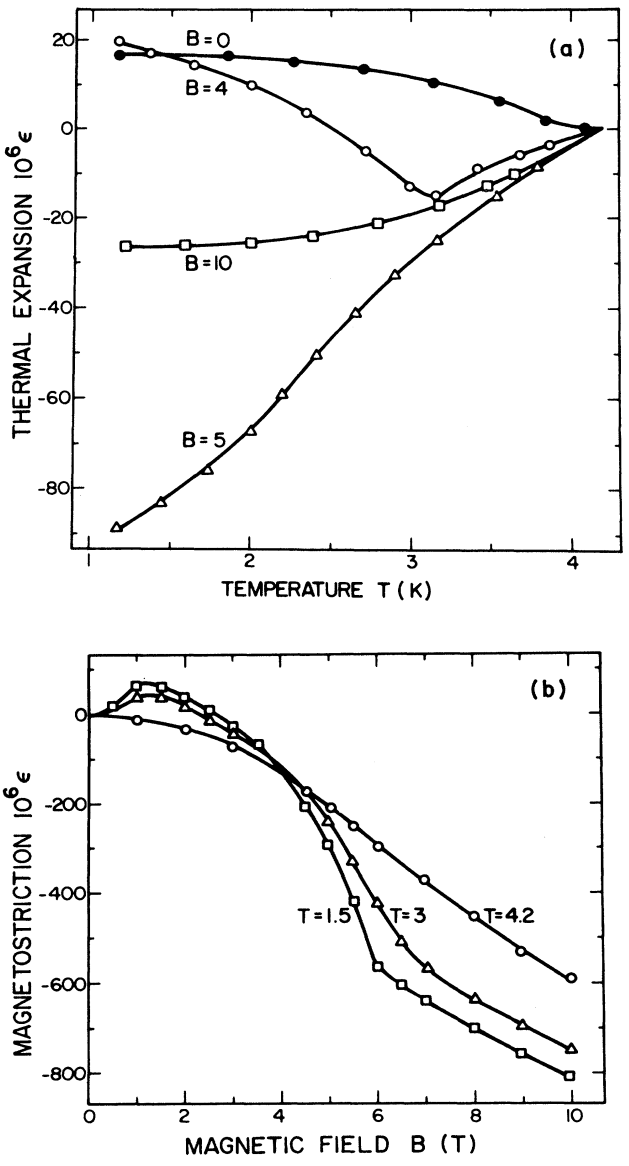

FIG. 6. (a) Thermal expansion of $CeAl_2$ with magnetic field B in units of T along a threefold symmetry axis and strain along a perpendicular twofold symmetry axis; (b) magnetostriction of $CeAl_2$ at temperatures T in units of K for the same configuration (line 5 of Table I).

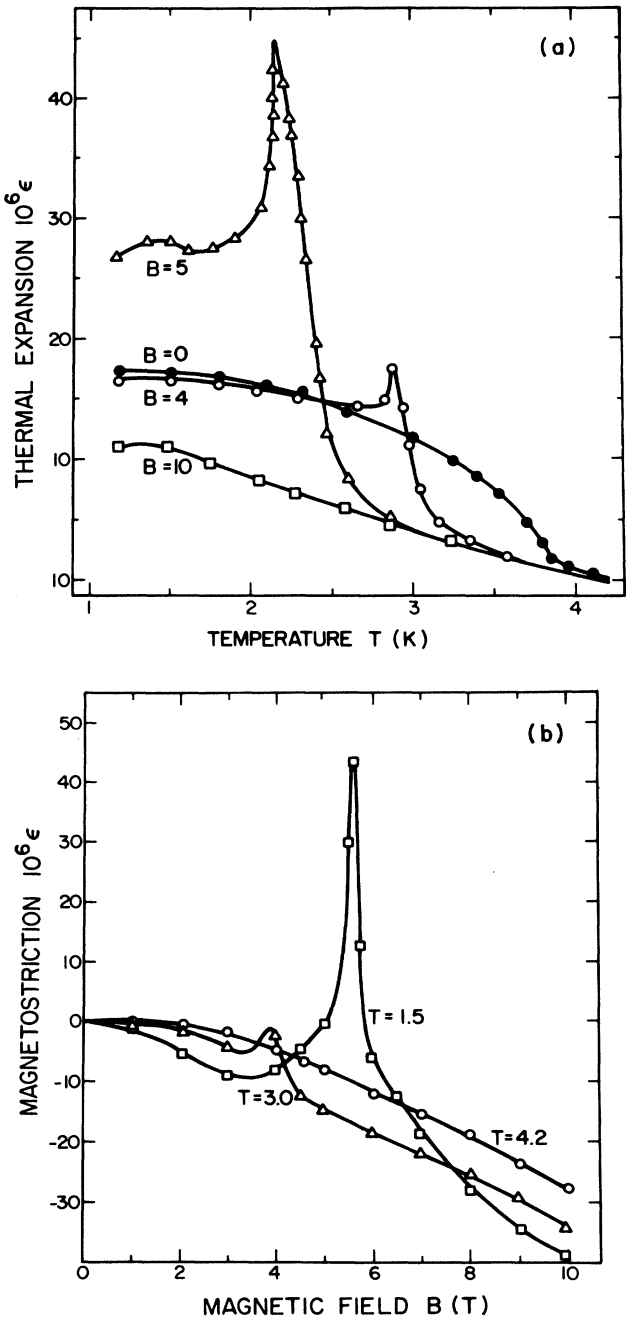

FIG. 7. (a) Thermal expansion of $CeAl_2$ with magnetic field B in units of T along a cube axis and strain along a twofold symmetry axis at angle $\pi/4$ to the field (line 6 of Table I); (b) magnetostriction of $CeAl_2$ at temperatures T in units of K with magnetic field along a cube axis and strain along a perpendicular twofold symmetry axis (line 7 of Table I).

The paramagnetostriction at temperature 4.2 K is described by the expression

$$\frac{\epsilon(B)}{B^2}=\frac{1}{B^2}\frac{\Delta l(B)}{l}$$
$$=\tfrac{1}{3}L_V+\tfrac{3}{2}L_{100}\sum_i \alpha_i^2\beta_i^2+3L_{111}\sum_{i\neq j}\alpha_i\alpha_j\beta_i\beta_j\ , \qquad (3)$$

where we have changed the notation of Averbuch and Segransan[22] so that the paramagnetostriction coefficients L_i correspond to the magnetostriction constants λ_i in Eq. (2). The magnetostriction at 4.2 K varies quadratically with magnetic field up to a field $B\simeq 4$ T to 5 T, but varies less rapidly at higher fields. We give in Table I the slope of the low-field quadratic plot for these various configurations of Figs. 1–7.

The procedure for evaluating L_i from the data in Table I by use of Eq. (3) follows that described above for the calculation of λ_i in the metamagnetic phase, except that L_{111} is calculated as the average of three values obtained from the values of the magnetostriction in lines 3, 4, and 5 of Table I, L_V having first been obtained from lines 2 and 7, and then L_{100} from line 1.

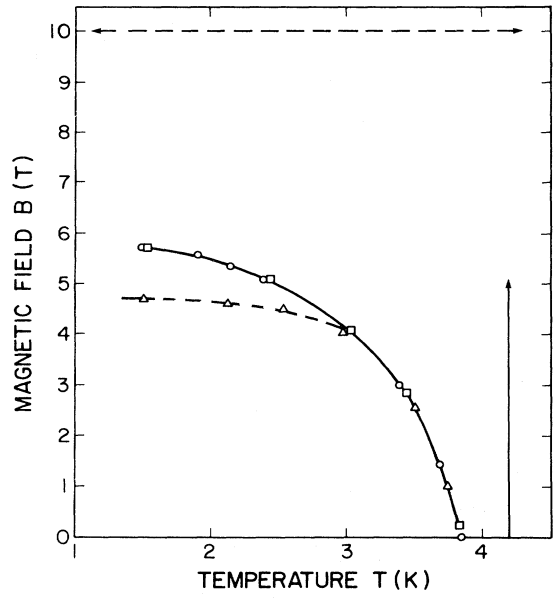

FIG. 8. Phase diagram of $CeAl_2$. The phase boundary between the antiferromagnetic phase and the high-field phase is determined for field along a cube axis (points o) by inflection points in the curve of Figs. 1(a) and 2(a) and similar curves at different temperatures and fields; for field along a twofold symmetry axis (points □) similarly from Figs. 4(a) and 4(b); and for field along a threefold symmetry axis (points Δ) similarly from Figs. 6(a) and 6(b). The arrow ↑ indicates the field range over which the paramagnetostriction coefficients L at temperature $T=4.2$ K were determined. The double-headed arrow (←– – –→) indicates the temperature range over which the magnetostriction constants λ_i in magnetic field, $B=10$ T, were determined, as shown in Fig. 9.

The resultant values

$$L_V=(-120\pm30)\times10^{-8}\ \mathrm{T}^{-2}\ ,$$
$$L_{100}=(230\pm30)\times10^{-8}\ \mathrm{T}^{-2}\ , \qquad (4)$$
$$L_{111}=(1520\pm230)\times10^{-8}\ \mathrm{T}^{-2}\ ,$$

should be compared with the values of the magnetostriction constants λ_i, also at temperature 4.2 K (see Fig. 9)

$$\lambda_V=-80\times10^{-6}\ ,$$
$$\lambda_{100}=145\times10^{-6}\ , \qquad (5)$$
$$\lambda_{111}=910\times10^{-6}\ .$$

The three values of λ_i are, within the experimental accuracy, in the same ratios as the values of L_i, and correspond when substituted into Eq. (3) to a fictitious internal field, $B_{\mathrm{int}}=7.9\pm0.2$ T. This agrees well with the value of 7.5 T for the molecular field associated with the Ce-Ce exchange interactions, which was estimated by Barbara *et al.*[23] from polarized neutron diffraction data.

The volume magnetostriction coefficient S_V may be calculated from the paramagnetostriction coefficients L_i by use of the equation[22]

$$S_V=\frac{\delta\omega(B)}{B^2}=\frac{1}{B^2}\frac{\Delta V(B)}{B}=L_V+\tfrac{3}{2}L_{100}+3L_{111}\ . \qquad (6)$$

The above values of L_i, when substituted in Eq. (6), give a volume magnetostriction for field directed along a cubic

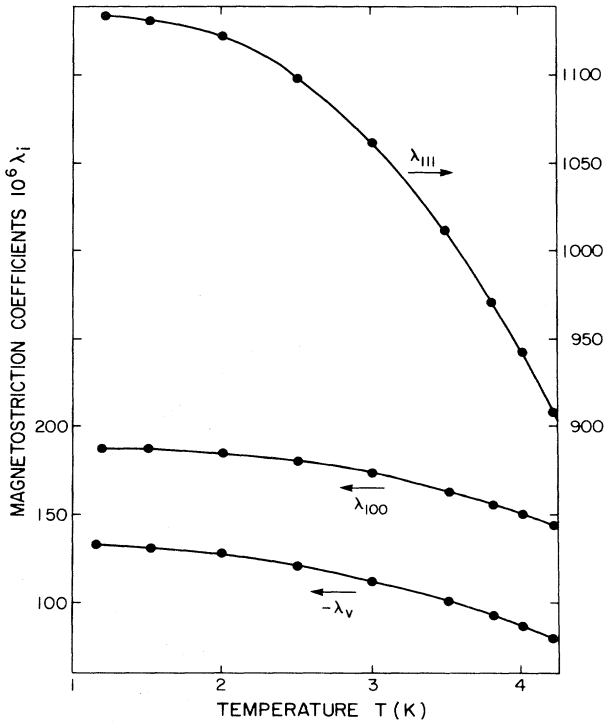

FIG. 9. Temperature dependence of the magnetostriction coefficients λ_i in the metamagnetic phase of $CeAl_2$ in a magnetic field, $B=10$ T.

axis, $S_V=(380\pm30)\times10^{-8}$ T^{-2}. Because of the enormous value of the trigonal shear coefficient L_{111}, the volume coefficient S_V^{pc} for a polycrystal[22]

$$S_V^{pc}=L_V+\tfrac{3}{2}L_{100}+3L_{111} \tag{7}$$

is considerably larger, $S_V^{pc}=(4800\pm700)\times10^{-8}$ T^{-2}.

The volume paramagnetostriction coefficient S_V gives[14] a magnetic Grüneisen parameter

$$\Omega_H=+\frac{d\ln\chi}{d\ln V}=\frac{2\mathcal{B}S_V}{\chi}=38\pm5 \tag{8}$$

by use of the value[24] $\mathcal{B}=70$ GPa for the low-temperature bulk modulus and the average peak value[11] of the susceptibility at about temperature 4 K, $\chi=(5.6\pm0.6)\times10^{-2}$ emu mol^{-1}.

This is to be compared with the values 12 (Refs. 8, 14, and B. Barbara, private communication) and 100,[25,14] obtained by measuring the pressure dependence of the susceptibility. The thermal Grüneisen parameter obtained from the pressure dependence of the linear term in the electronic specific heat, measured by Berton *et al.*[8]

$$\Omega_T=+\frac{d\ln\gamma}{d\ln V} \tag{9}$$

is opposite in sign, with the value -40.[14] We note, however, that the positive signs in the definitions of Ω_H and Ω_T in Eqs. (8) and (9), while being appropriate for a system like a transition metal in which both χ and γ are inversely proportional to a band energy,[14] may be inappropriate for a heavy-fermion system like $CeAl_2$.

The reason for the large magnetic Grüneisen parameter observed in many heavy-fermion systems[26] is believed to be that the spin-fluctuation temperature, which is equivalent to the single-ion Kondo temperature, depends exponentially on the volume-dependent hybridization of the magnetic ion with the surrounding conduction electrons.[27] In $CeAl_2$ however, while the various volume Grüneisen parameters are all large,[14] the values of the magnetostriction constants λ_i in Eq. (5) show that the shear deformation associated with the antiferromagnetic order is an order of magnitude larger than the volume strain.

A small amount of hysteresis is observed in the antiferromagnetic phase at low fields and temperatures, especially when the field is applied along a twofold symmetry axis. This is illustrated in the insert to Fig. 4(b), but in other cases where the hysteresis is even smaller, or is not observed at all, we show only the behavior for increasing field. Such hysteresis is to be expected in a situation where there is domain-wall motion, as some antiferromagnetic domains grow at the expense of others with changing field, due to magnetic anisotropy.

It is most surprising however to observe pronounced hysteresis at temperature 4.2 K, where we would expect $CeAl_2$ to be a paramagnet with no long-range order. The behavior illustrated in Fig. 10 may be due to stress imposed on the sample by the differential thermal contraction with respect to the beryllium-copper base plate to which it is glued, which induces some part of it to become antiferromagnetic at temperature 4.2 K, about 0.4 K above the normal Néel temperature. The hysteresis would be associated with antiferromagnetic domain-wall motion, and it is interesting to note that the effects are particularly pronounced when the field is along a twofold symmetry axis, which is similar to the behavior at low temperatures, as illustrated in Fig. 4(b). We note however that for other field directions there may be similar hysteresis, especially when the field is first applied after cooling, but only the hysteretic behavior for the configuration shown in Fig. 10 was recorded, because of the large size of the effect in this case.

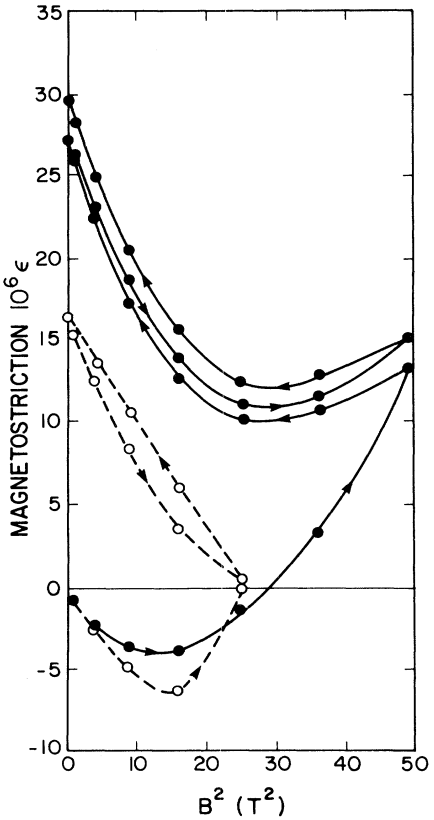

FIG. 10. Hysteresis in the magnetostriction of $CeAl_2$ at temperature 4.2 K with magnetic field along a twofold symmetry axis and strain along a perpendicular cube axis. The dashed curves through open circles and the solid curves through solid circles correspond to different runs, between which the sample was brought to room temperature.

CONCLUSION

The strong anisotropy of the large magnetoelastic coupling in $CeAl_2$ makes the present study on single-crystal samples especially interesting. The very large magnitude of the trigonal shear magnetoelastic constant deserves

theoretical study. The similarity between the relative magnitudes of the magnetoelastic constants, which characterize the changes in strain deformation between the zero-field antiferromagnetic state and the metamagnetic state, and the paramagnetic coefficients, is also worth remarking.

ACKNOWLEDGMENTS

This work was supported by the Natural Sciences and Engineering Council of Canada and was performed in Toronto during separate visits by two of the authors (V. P. and H. K.)

[1]S. Doniach, Physica **91B**, 231 (1977).

[2]C. D. Bredl, F. Steglich, and K. D. Schotte, Z. Phys. B **29**, 327 (1978).

[3]B. Barbara, M. F. Rossignol, H. G. Purwins, and E. Walker, Solid State Commun. **17**, 1525 (1975).

[4]F. Steglich, C. D. Bredl, M. Loewenhaupt, and K. D. Schotte, J. Phys. (Paris) **40-C5**, 301 (1979).

[5]B. Barbara, J. X. Boucherle, J. L. Buevoz, and J. Schwedizer, J. Phys. (Paris) **40-C5**, 321 (1979).

[6]B. Barbara, M. F. Rossignol, J. X. Boucherle, and C. Vettier, Phys. Rev. Lett. **45**, 938 (1980).

[7]B. Luthi and C. Lingner, Z. Phys. **34**, 157 (1979).

[8]A. Berton, J. Chaussy, G. Choutdeau, B. Cornut, J. Floquet, J. Odin, J. Palleau, J. Peyrard, and R. Tournier, J. Phys. (Paris) **40-C5**, 326 (1979).

[9]B. Barbara, M. Cyrot, C. Lacroix-Lyon-Caen, and M. F. Rossignol, J. Phys. (Paris) **40-C5**, 340 (1979).

[10]R. Schefzyk, W. Lieke, and F. Steglich, Solid State Commun. **54**, 525 (1985).

[11]M. C. Croft, I. Zoric, and R. D. Parks, Phys. Rev. B **18**, 5065 (1978).

[12]M. C. Croft, I. Zoric, and R. D. Parks, Phys. Rev. B **18**, 345 (1978).

[13]E. Walker, H. G. Purwins, M. Landolt, and F. Hullinger, J. Less Common Met. **33**, 203 (1973).

[14]E. Fawcett, Solid State Commun. **71**, 853 (1989).

[15]V. V. Moshchalkov, P. Coleridge, E. Fawcett, and A. Sachrada, Solid State Commun. **60**, 893 (1986).

[16]F. Lapierre, P. Haen, A. Briggs, and M. Sera, J. Magn. Magn. Mater. **63-64**, 76 (1987).

[17]U. Welp, G. Bauls, G. Remenyi, P. Haen, A. Briggis, J. Flouquet, P. Morin, G. Cors, and M. Karkut, J. Magn. Magn. Mater. **63-64**, 28 (1987).

[18]B. Cornut and B. Coqblin, Phys. Rev. **11**, 845 (1972); Y. Lassaily, A. K. Bhattacharjee, and B. Coqblin, Phys. Rev. B **31**, 7424 (1985).

[19]The boule was supplied by Dr. G. Crabtree, and a resistivity sample cut from the same boule was used in the work described in Ref. 15.

[20]G. K. White and J. G. Collins, J. Low Temp. Phys. **7**, 43 (1972).

[21]R. Becker and W. Doring, *Ferromagnetismus* (Springer, Berlin, 1939).

[22]P. G. Averbuch and P. J. Segransan, Phys. Rev. B **4**, 2067 (1971).

[23]B. Barbara, J. X. Boucherle, M. F. Rossignol, and J. Schweizer, Solid State Commun. **24**, 481 (1977).

[24]T. Penney, R. Barbara, T. S. Plasket, H. E. King, Jr., and S. J. LaPlaca, Solid State Commun. **44**, 1199 (1982).

[25]M. C. Croft, R. P. Guertin, L. C. Kupferberg, and R. P. Parks, Phys. Rev. B **20**, 2073 (1979).

[26]B. Luthi, J. Magn. Magn. Mater. **52**, 70 (1985).

[27]P. Fulde, J. Keller, and G. Zwicknagl, Solid State Phys. **42**, 1 (1988).